Proceedings of the SDR 11 Technical Conference and Product Exposition,

A LOW-COST GNSS-R SYSTEM BASED ON SOFTWARE-DEFINED-RADIO

Thomas Hobiger, Jun Amagai, Masanori Aida, Hideki Narita, and Tadahiro Gotoh
(National Institute of Information and Communications Technology,
Koganei, Tokyo, Japan)

ABSTRACT

Global Navigation Satellite Systems (GNSS) signals can be utilized to implement a passive-radar system using ground or sea surface reflections. Analysis of delay and Doppler characteristics of these reflections allows to derive physical parameters of the reflecting area. Supported by software defined radio the development of a flexible GNSS-R system, which is capable to handle the whole signal processing chain on an off-the-shelf PC, becomes possible. The usage of graphic processing units (GPUs) even allows real-time operation of the system and helps to reduce the development and operational cost to a minimum. Moreover, future GNSS signals and satellite systems can be supported easily by adopting the software modules as well as innovative processing algorithms can be implemented and tested.

1. INTRODUCTION

GNSS-Reflectometry (GNSS-R) is a new emerging application that utilizes signals from navigation satellites. Other than classical GNSS applications, the received signals are not used to determine position, velocity or time of the receiver, nor are they processed to provide information about the atmosphere or ionosphere. GNSS signals are transmitted from satellites and are usually expected to be received by a ground based antenna, avoiding multi-path or reflections in order to achieve utmost high precision positioning results. Nevertheless, for a variety of applications (e.g. [1]) the information from reflected signals can become a valuable data source, from which one can deduce (geo-) physical properties. Since most GNSS antennas are designed to receive only the direct, i.e. right-hand circular polarized (RHCP) signals, it is necessary to deploy a dedicated antenna which is capable to detect the reflected signals which have changed to left-hand circular polarization (LHCP) after being reflected. Moreover, in most of the cases GNSS-R antennas are not pointed towards the sky, but either looking downwards or at least being tilted towards the horizon in order to receive the reflected signals within the main lobe of the antenna beam pattern. Depending on the application and the area of interest, GNSS-R systems can be mounted close to the ground (e.g. [2]), flown on an airplane (e.g. [3]) or even installed on board of a satellite (e.g. [4]). In order to measure instrumental delay changes due to platform movement or instrumental characteristics it is common to utilize two GNSS antennas, whereas one is dedicated to track direct RHCP GNSS signals and the other one is assigned to receive the reflected LHCP signals. Such a GNSS-R system is not only capable to measure the reflection characteristics but also turns into an altimeter when arrival times of direct and reflected signals are being compared. Additionally, a comparison of RHCP and LHCP signal strength allows to derive the attenuation caused by surface reflection and excess path.

2. GNSS-R ANTENNA

Two commodity active GNSS antennas, one RHCP and one LHCP type were mounted on a two meter pole. In order to avoid that a signal can enter both antennas, two disk shaped aluminum plates are placed below each antenna. Figure 1 depicts a photo-realistic rendering of the pole with the two GNSS antennas mounted on the head, whereas the RHCP type is intended to be oriented toward zenith in order to receive the direct signals. The LHCP antenna on the opposite site is sensitive to reflected waves from the ground or objects below. Antenna cables with identical electrical

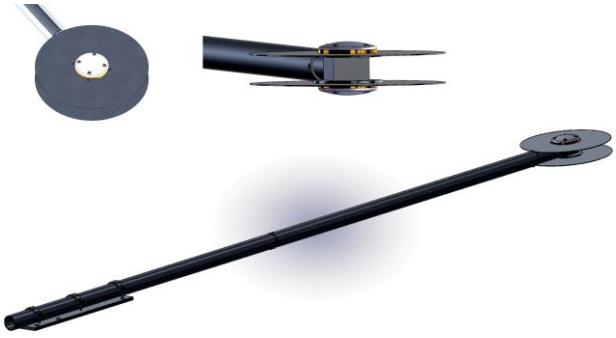

Figure 1: RHCP and LHCP GNSS antennas separated by two aluminum disks and mounted on a two meter pole. Cables leading to the antennas are inside the pole.

length are guided inside the pole.

3. GNSS-R FRONT-END BASED ON ETTUS USRP2

All modern GNSS are transmitting their civil and/or military signals in L-band whereas most of the systems facilitate at least two different frequencies in order to remove dispersive delay effects caused by trans-ionospheric propagation. Therefore a receiver front-end must be flexible enough to cover a wide range of L-band frequencies as well as support a wide-enough bandwidth to capture the spread-spectrum signals. The USRP2 sold by Ettus Research LLC [5] as main platform and the DBSRX2 daughterboard fulfill these requirements and allows direct sampling of any concerned GNSS signal without the need for additional down-conversion or filtering. Center frequencies, sampling bandwidth and gain factors can be controlled from a PC which also receives the sampled data-stream from the device via a standard Gigabit Ethernet connection using the UDP protocol. Figure 2 depicts the signal flow from the antenna to the PC using two USRP2 units which are connected by a so-called MIMO cable. This cable allows to stream the sampled data from a slave USRP2 device to the master device before both data streams are merged and sent as UDP packets. As a second feature, which is crucial for a GNSS-R system, the MIMO cable syncronizes the internal oscillator frequencies and sampling intervals between both USRP2s. This ensures that both devices sample the RF signals at the same center frequencies and epoch. Since GNSS-R measurements are differential measurements external 10 MHz and 1 PPS signals are not necessary to keep the devices syncronized w.r.t an absolute reference.

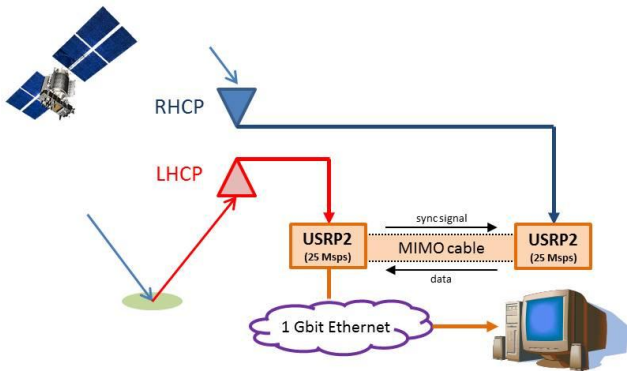

Figure 2: USRP2 hardware front-end and the signal flow to the processing PC. The MIMO cable between the two USRP2 units carries out the data transfer from the slave device and synchronizes both devices to operate with the same oscillator frequency.

4. GNSS-R SOFTWARE RECEIVER

Processing of the sampled RHCP and LHCP signals requires sophisticated methods as well as a computing platform which is capable of ensuring to run the GNSS-R system in real-time. Based on the experience gained with graphics processing units (GPUs) for implementing a software GPS receiver [6] the choice was made to use this parallel platform again for the challenging task to process large amount of data in real-time. Thereby, the GNSS-R system can be split into three modules (figure 3) which are described in the following three subsections.

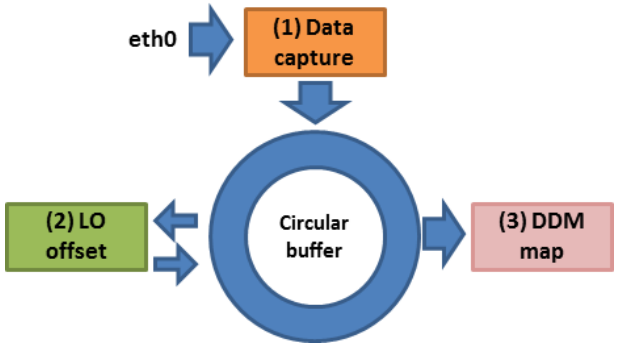

Figure 3: Interaction of the software receiver modules which run as independent processes on a single PC and exchange data via a circular buffer in shared memory.

4.1. Data capture module

The first of the three modules (see figure 4) runs entirely the CPU and is dedicated to listen to the Ethernet port and decodes the incoming UDP packets into the sampled data streams of the RHCP and LHCP data. It outputs these samplings together with time tag information to a large circular buffer which is realized in global shared memory. Thus, the data becomes accessible to different CPU processes which can run independently from this module. Sampling rate and the PC's memory size allow data to be kept in the circular buffer spanning a few seconds up to almost one minute. For the initial field tests an off-the-shelf PC has been equipped with 16 GB of RAM to allow for higher sampling rates without overwriting unprocessed data in the memory.

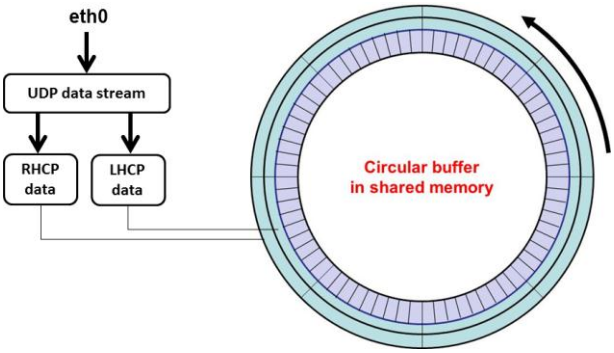

Figure 4: Data capture module.

4.2. Local oscillator offset determination

The second module basically runs a GNSS software receiver as described in [6] based on the RHCP data stream. In order to make sure that this computational intensive module does not interfere with other real-time modules the entire processing takes place on a GPU. Thereby, all visible GNSS satellites above the local horizon are tracked continuously and code delay, code phase and amplitudes are determined. As depicted in figure 5, every 32 millisecond the phases are used to update the Doppler tracking loop (for details see [6]) and results are copied back to the CPU. The obtained Doppler values are compared with theoretical ones based on broadcast orbit information and site position. The difference between the observed Doppler values and those theoretical ones equal to the local oscillator offset of the sampler (i.e. the USRP2). A robust estimate for this offset can be obtained by computing a weighted average over all visible satellites at a given epoch. The obtained LO offset information is then aligned with the time tags and is written to the circular buffer, keeping the rest of the raw data unchanged.

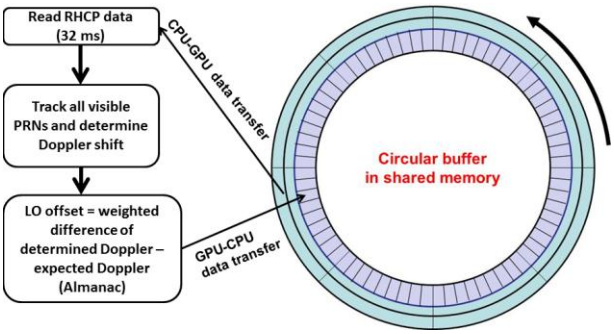

Figure 5: LO offset determination module.

Besides continuous tracking of the local oscillator w.r.t. the nominal frequency, this module provides also the navigation bit status for each visible satellite. Most GNSS modulate navigation messages on their ranging signal by a CDMA spread-spectrum technique [7]. Therefore, phase jumps of ±180 degrees can be seen every time the navigation bit status changes. Thus, coherent integration (as applied in the third module, see section 4.3) over time-spans longer than one navigation bit is only feasible if the navigation bit status is known for each satellite that is being processed by the GNSS-R module (see next section).

4.3. Delay-Doppler map generation

The last of the three software modules is the core part of the GNSS-R software radio as it provides the reflectometry related information based on the direct and reflected signals. This computational intensive part modules runs also on a GPU. Considering that also the LO module (section 4.2) runs on a GPU, in total two graphic cards are required for PC operating the complete GNSS-R system. Once RHCP and LHCP data are transferred to GPU memory, signals are mixed-down with the corrected LO offset information and compared against replica codes of the GNSS satellites (see figure 7). As this comparison is done in time and spectral domain, a 2D cross-correlation map can be obtained in delay and Doppler shift direction after performing 2D FFT operations as described in [8]. In order to accumulate i.e. coherently integrate, data over time-scales longer than one

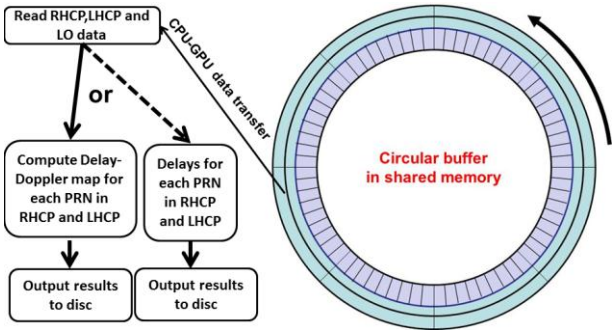

Figure 6: Delay-Doppler map module.

navigation bit (usually 20 milliseconds) it is necessary to apply the 180 degree phase changes detected from the LO offset module (see section 4.2). Additionally obtained Delay-Doppler maps (DDM) can be stacked, i.e. incoherently integrated, in order to increase the signal-to-noise ratio (SNR) if necessary. DDM generation makes use of the massive computing performance of the GPU and computes all RHCP and LHCP DDMs in parallel. Depending whether incoherent integration is applied or not, the generated maps are copied back from GPU memory to the CPU where they are finally kept into CPU memory for further processing or stored on the hard disc in binary format.

The DDM module can run in an second mode where only delay information is extracted from the RHCP and LHCP data streams.

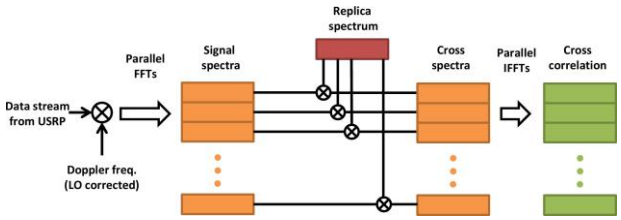

Figure 7: Architectural diagram of the DDM module. The incoming data stream is mixed down with the corresponding Doppler frequency (corrected for the LO offset) and parallel FFTs are performed over several milliseconds of data. Thereafter, signal and replica spectra are multiplied in the frequency domain and parallel IFFTs provide cross-correlation functions each millisecond. This information can be used to derive delay-only information (by searching the peak of each cross-correlation function) or applied to generate DDMs by a 2D FFT operation.

4.4. Post-processing

The DDMs can be processed in real-time if the remaining CPU resources of the PC don't interfere with the GNSS-R modules. Otherwise data can also be streamed to another PC or stored on the hard-disk for off-line processing. Depending on the location of the GNSS-R antenna and the type of reflecting surface different geophysical parameters can be extracted. For ground based systems, the Doppler pattern of the LHCP data does not differ much from the RHCP data and thus delay and amplitude information can be used only. Moreover, as ground reflections from e.g. soil are weak, phase information of the reflected signal is in most cases not usable. Reflections from water or snow lead to less attenuation of the LHCP signals and thus allow to analyze the relative phase between direct and reflected wave fronts yielding millimeter accurate delay information which can be used to monitor surface deformations [9]. Moreover, a comparison of signals amplitudes of the LHCP w.r.t the RHCP provides valuable information about the attenuation due to reflection at a given point. Paired with a proper physical model, this information can be used to derive geophysical parameters like soil moisture [10]. For the case that the GNSS-R receiver is located high above the ground, the Fresnel zone [11] of the reflected area is large enough so that the Doppler pattern of the LHCP data shows a significant difference w.r.t. the direct RHCP signal. As discussed e.g. in [12] one can use this to fit various geophysical parameters from the two-dimensional DDMs.

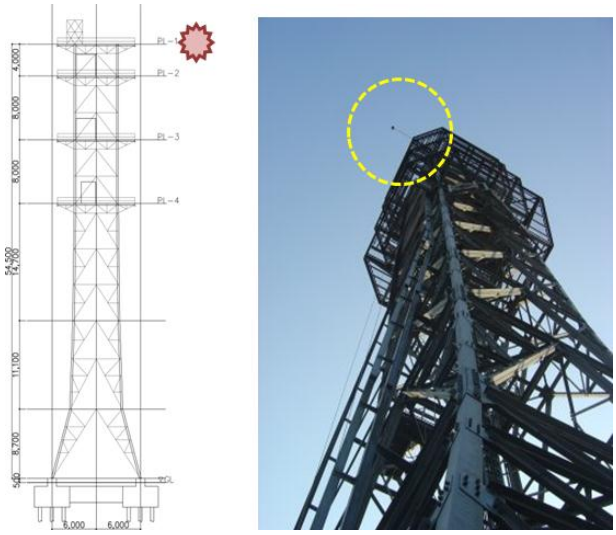

Figure 8: Location for the initial field tests of the prototype GNSS-R system. The antenna pole (red star in left figure, marked by a circle in the right picture) has been put on top of a 55m high steel tower located at NICT's headquarter in Tokyo. The hardware frontend and the processing PC are hosted in a container on a platform below the top level.

5. TEST SITE

In order to test the proto-type system a place high enough to receive meaningful reflections but also close enough for debugging the system via a fast internet connection was required. Such a place has been found by a 55 m high telecommunication tower inside NICT's headquarter in Koganei, Tokyo (figure 7). As the tower also hosts an air-conditioned container, the power supply, RF front-ends and the processing PC could be placed there. A fast internet connection allows remote control of the system and data download for post-processing purposes.

6. RESULTS

After deployment and installation of the system on top of the steel tower (see prior section) was completed an initial 12h test of the GNSS-R system was carried out. Caused by the local environmental conditions, only reflections from Eastward directions can be captured as the steel tower is blocking the line-of-sight for reflections from the Western area. Nevertheless, these circumstances have been already anticipated when selecting the location for the initial field tests and as Eastward of the tower a large agricultural training field of a nearby university exists, reflections from different ground conditions are expected to be visible in the received data. On February 20th, 2011 a 12h test was carried out and results from this experiment are discussed in the following.

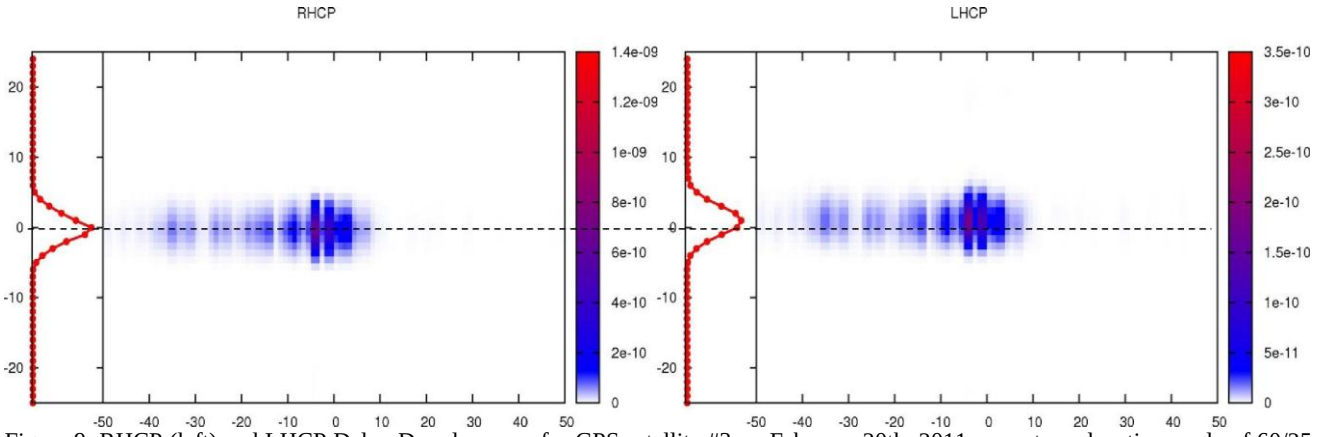

Figure 9: RHCP (left) and LHCP Delay-Doppler maps for GPS satellite #3 on February 20th, 2011 seen at an elevation angle of 60/25 degree. Horizontal axes represent Doppler shifts and vertical axes reflect delay shifts. Signals amplitudes are shown in arbitrary linear units but are consistent between both maps. A dotted line has been added to clarify the delay caused by the extra path delay due to reflection.

6.1. Example: Delay-Doppler maps and related information

Using a coherent integration time of 2.048 seconds Delay-Doppler maps were computed in real-time and stored on the PC for off-line processing. After the experiment finished, the binary DDMs were downloaded and analyzed. As an example, figure 8 shows RHCP and LHCP maps for a given epoch and satellite. As anticipated (see discussion in section 4.4) the Doppler pattern does not differ much between the direct and reflected DDM since the height of the tower does not create a large Fresnel zone which could lead to a significant change of the Doppler characteristic. Nevertheless, two main features could be observed. First, the peak the LHCP DDM is shifted in delay direction w.r.t. the RHCP map. This shift equals the delay due to the extra path length δ which can be described by

$$\delta = 2\ h\ \sin(\beta) \qquad (1)$$

where h equals the height of the GNSS-R above the reflecting surface and β represents the elevation angle under which the satellite is seen on the ground point. Integration over all Doppler bins reveals the typical triangular shaped GNSS correction function, which depicts this delay even more pronounced than one can see by naked eye from the two-dimensional DDMs. As a second feature it can be noticed that the amplitude of the reflected signal is lower (by about 6 dB) than those of the direct RHCP signal. Thus the attenuation coefficient due to reflection can be deduced for each ground point. Overall it can be noticed that the DDM pattern of both signals is slightly skewed towards negative Doppler shifts which can be explained by applying a LO offset correction that does not totally reflect the true physical oscillator frequency of the sampler. Nevertheless, since the same LO offset value is used to mix down the RHCP and LHCP data streams the relative information extracted from both maps will be unaffected by this imperfectness.

6.2. Altimetric results

As described in the prior section, the LHCP DDM is shifted w.r.t. the RHCP map by a small delay δ that originates from the additional path length which the LHCP signal takes before it reaches the antenna. Using the basic equation (1) and computing the observing geometry, based on a-priori station coordinates and orbit parameters, one can determine

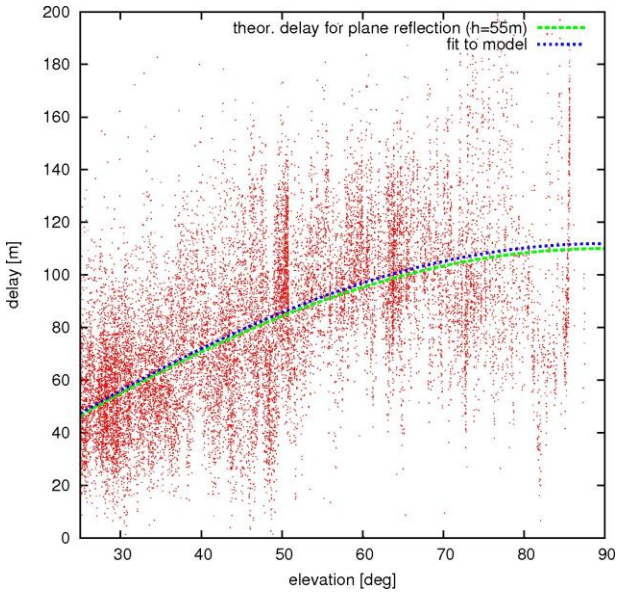

Figure 10: Measured delays between LHCP and RHCP antenna over 12 hours for different elevation angles. A theoretical model for the delays (green line) based on a tower height of 55 meter matches well with a fit (blue line) through

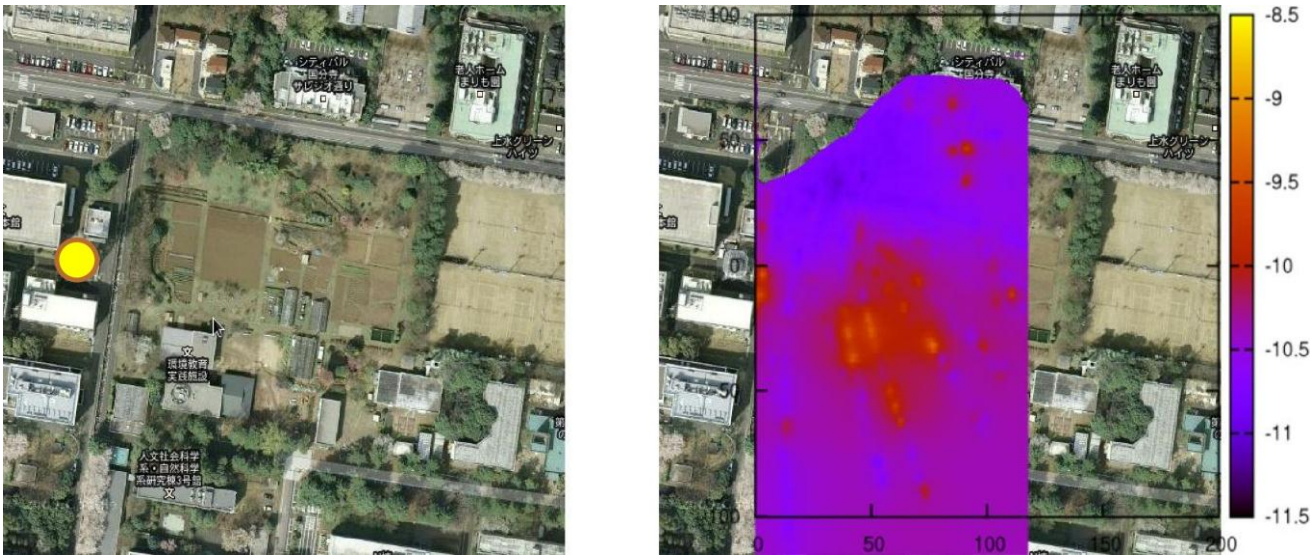

Figure 11: Left image: Location of the GNSS-R system in Koganei, Tokyo. The yellow dot represents the location of the 55m tower on which the system is mounted. Fields from a neighboring university in the East as well as small building in the South East area are a good test scenario for the system in an urban environment. Right image: Radiometric measurement, i.e. signal strength LHCP vs. RHCP, are assigned to the reflecting points on the ground and spatially interpolated. Reflections from building can be clearly identified as areas with less attenuation, since the metal roofs act as better reflecting surfaces than soil from the fields. (Note: areal images are taken from Google Maps™)

the height of the antenna above the reflector. In order to obtain best estimates of δ from each RHCP/LHCP DDM pair the following delay extraction method has been applied to the 12h data set:

1. Compute the 2D FFT of each DDM.
2. Take the complex conjugate of the LHCP transform
3. Multiply both maps in the Fourier domain
4. Apply an inverse 2D to this map
5. Sum over all bins in Doppler direction, providing the cross-correlation function in delay direction
6. Since the resolution is limited by the sampling rate of the system, a Gaussian curve is fitted through the cross-correlation function.
7. The location of the peak of the Gaussian curve equals the observed relative delay δ.

By using this approach, a robust and automated extraction of delay information could be realized. Figure 9 shows the obtained delays from the 12h data-set together with a theoretical model based on a flat two-dimensional reflecting surface. If the GNSS-R would be located above an ideal flat ground one would expect to measure results close to the theoretical model only. But since the antenna has been mounted in an urban area, reflections not only from the nearby field, but also from buildings and other objects can be seen in the measurements.

6.3. Radiometric results

Comparison of amplitudes of LHCP and RHCP DDMs allows to derive the attenuation factor that the corresponding ground reflection causes to the signal. Since the GNSS ground-tracks are varying with time, a large area can be covered with this information if data from longer time spans are accumulated. Based on the 12 hour data-set, a map has been generated, which shows the attenuation factors as a two-dimensional map around the tower on which the GNSS-R system is placed. A clear spatial pattern can be seen in this map (figure 10), whereas strong reflection from roofs appear as areas of less attenuation. Since the ground tracks were geo-referenced w.r.t. a flat surface instead of modeling the building with their correct height, reflections from these objects appear to be closer to the tower and thus are not totally coinciding with the locations of these buildings. This can be improved in future if a realistic terrain model is applied for plotting the location of the reflecting points.

7. SUMMARY

Software-defined radio enabled the development of a flexible and low-cost GNSS-R system that can be utilized for a variety of application. Using only off-the-shelf components together with the USRP2 technology led to a robust and easy to handle system which can even be designed by experts from other fields than electronic engineering. First field tests in an urban area confirmed the

system concept, and altimetric and radiometric measurements agree well with the environmental settings that lead to ground reflections around the test site. Other than FPGA based GNSS-R solutions, this system can be extended easily to adopt new signals or to test new processing algorithms. Thus, beside operational use, software defined radio allows also to use this system for educational and development purposes.

8. OUTLOOK

Since the system concept of the software defined GNSS-R radio could be confirmed, longer test runs are currently under way. This will help to remove minor bugs in the processing chain and enables testing of new or improved algorithms. Moreover it is anticipated that a denser map of ground reflections can be obtained as well as that time-dependent variations become visible. Thus, e.g. rain or snow dependent changes of reflectivity should become clearly visible in such time-series. Tests runs over longer periods should also be able to reveal soil moisture changes in the nearby fields. The current limitation of the maximum sampling rate (i.e. 12.5 Msps) can be overcome by using unsigned short integer I/Q data streams instead of the single precision floating point representation. Therefor it has to be studied how much the processing overhead due to data conversation and extension of the sampling rate to 25 Msps would cause and if real-time processing can be still ensured. In the close future it is anticipated that the system is being located at a coastal site for sea level measurement or sea state monitoring. Since the reflections from water appear as much stronger signals and phase measurements can be utilized the accuracy of the system is expected to reach mm-level, which would make it a cheap and valuable tool for a variety of oceanic and geodetic applications. Moreover, the developed system can be mounted on a vessel or inside an airplane in order measure sea state parameters either close to the surface or from several kilometers above. The latter application would also reveal the full potential of the information contained in the Delay-Doppler maps, as the reflection pattern can be assigned to e.g. sea surface roughness which allows to deduce wind parameters or other geophysical signals.

9. ACKNOWLEDGMENTS

This work was supported by a NICT Incentive Fund for the year 2010. The authors like to thank NICT's trial manufacture development team for the construction of the antenna pole as well as for supporting the installation on top of the 55 m tower. Various NICT groups are acknowledged for the provision of a high-speed fiber connection which allows to remotely operate the system from the ground.

10. REFERENCES

[1] A. Egido, M. Delas, M. Garcia, and M. Caparrini, Non-space applications of GNSS-R: From research to operational services. Examples of water and land monitoring systems, *Geoscience and Remote Sensing Symposium, 2009 IEEE International, IGARSS 2009* , vol. 2, pp.II-170-II-173, 12-17 July 2009

[2] X. Zhang, X. Wang, L. Shao, Q. Sun, X. Hu, L. Xu, G. Ruffini, D. Stephen, and F. Soulat, First results of GNSS-R coastal experiment in China, *Geoscience and Remote Sensing Symposium, 2007, IGARSS 2007. IEEE International*, pp. 5088-5092, 23-28 July 2007.

[3] G. Ruffini, F. Soulat, M. Caparrini, O. Germain, and M. Martin-Neira, The Eddy Experiment: Accurate GNSS-R ocean altimetry from low altitude aircraft, *Geophys. Res. Lett.*, vol. 31, L12306, 2004.

[4] M.P. Clarizia, C. Gommenginger, S. Gleason, C. Galdi, and M. Unwin, Global Navigation Satellite System-Reflectometry (GNSS-R) from the UK-DMC Satellite for Remote Sensing of the Ocean Surface, *Geoscience and Remote Sensing Symposium, 2008. IGARSS 2008. IEEE International* , pp.I-276-I-279, 7-11 July 2008.

[5] Ettus Research LLC, http://www.ettus.com

[6] T. Hobiger, T. Gotoh, J. Amagai, Y. Koyama, and T. Kondo, A GPU based real-time GPS software receiver, GPS Solutions, vol. 14, no. 2, pp. 207-216, 2010.

[7] E.D. Kaplan, *Understanding GPS: principles and applications*, Artech House Publishers, Boston/London, 1996.

[8] S. Gleason, S. Hodgart, S. Yiping, C. Gommenginger, S. Mackin, M. Adjrad, M. Unwin, Detection and Processing of bistatically reflected GPS signals from low Earth orbit for the purpose of ocean remote sensing, *IEEE Transactions on Geoscience and Remote Sensing*, vol. 43, no. 2, pp. 1229-1241, 2005.

[9] A.M. Semmling et al., Detection of Arctic Ocean tides using interferometric GNSS-R signals, *Geophys. Res. Lett.*, vol. 38, L04103, 2010.

[10] N. Rodriguez-Alvarez et al., Land Geophysical Parameters Retrieval Using the Interference Pattern GNSS-R Technique, *Geoscience and Remote Sensing, IEEE Transactions on*, vol.49, no.1, pp.71-84, Jan. 2011.

[11] P. Ferrazzoli, L. Guerriero, N. Pierdicca, and R. Rahmoune, Forest biomass monitoring with GNSS-R: Theoretical simulations, *Advances in Space Research*, vol. 47, no. 10, pp. 1823-1832, 17 May 2011.

[12] O. Germain, G. Ruffini, F. Soulat, M. Caparrini, B. Chapron, and P. Silvestrin, The Eddy Experiment: GPS speculometry for directional sea-roughness retrieval from low-altitude aircraft, *Geophys. Res. Lett.*, vol.31, L21307, 2004.